

Angular Baryon Acoustic Oscillation measure at $z=2.225$ from the SDSS quasar survey

E. de Carvalho^{1,2,*}, A. Bernui^{1,†}, G. C. Carvalho^{1,‡} and C. P. Novaes^{1,§}

¹*Observatório Nacional, 20921-400, Rio de Janeiro, RJ, Brazil and*

²*Universidade do Estado do Amazonas, 69640-000, Tabatinga, AM, Brazil*

(Dated: December 14, 2024)

The Baryon Acoustic Oscillation (BAO) phenomenon imprinted a characteristic scale to the spatial distribution of matter. Traditionally, one assumes a fiducial cosmology to compute the comoving distance among pairs, then the characteristic scale is determined through the three-dimensional two-point correlation function. Here we follow a quasi model-independent approach to measure the transversal BAO mode at high redshift using the two-point angular correlation function (2PACF). This analysis is only possible now with the quasars catalog from the twelfth data release (DR12Q) from the Sloan collaboration, because it is dense enough (in redshift space) to measure the angular BAO signature with high statistical significance and acceptable precision. Our analyses considering quasars in the redshift interval $z \in [2.20, 2.25]$ produced the angular BAO scale $\theta_{\text{BAO}} = 1.85^\circ \pm 0.33^\circ$ with a statistical significance of 3.8σ . Additionally, we show that the BAO signal is robust under tests using different numbers of random catalogs used in the calculation of the 2PACF, and is also stable under diverse bin-size choices. Finally, we also performed cosmological parameter analyses comparing the θ_{BAO} predictions for the models Λ CDM and $w(a)$ CDM with angular BAO data available in the literature, including the measurement obtained here, jointly with CMB data. The constraints on the parameters Ω_M , w_0 and w_a are in excellent agreement with the Λ CDM concordance model.

I. INTRODUCTION

One of the most iconic and incomprehensible components of the universe is the *dark energy*, an unknown entity representing $\sim 70\%$ of the cosmos [1]. A powerful approach to unveil the dark energy mysteries is searching for the Baryon Acoustic Oscillations (BAO) signature at different epochs to probe its time evolution [2–7].

The BAO is a primordial phenomenon that imprinted a characteristic scale, the sound horizon r_s , in the spatial distribution of cosmic objects. Almost a decade of success mapping the large-scale distribution of luminous matter provided large, dense, and deep surveys of cosmological tracers of the universe evolution like luminous red galaxies, emission line galaxies, and quasars [8–10]. With these data, analyses of the two-point correlation function (2PCF) produced robust detections of the BAO signature in different data ensembles giving precise measurements of the distance-redshift relationship, mainly using luminous red galaxies [11–13], but also with clusters of galaxies [14, 15].

Moreover, to probe the early time evolution of the dark energy it is imperative to investigate the highest redshift available cosmological tracer, that is, the quasars [16–18]. The first BAO analyses with quasars, $2.1 \leq z \leq 3.5$, started in 2013 using the data release 9 (DR9) of the Baryon Oscillation Spectroscopic Survey, part of the Sloan Digital Sky Survey (SDSS) [8], which

measured the BAO features in the three-dimensional correlation function in the Lyman- α flux fluctuations resulting in constraints on the angular diameter distance, D_A , and the Hubble expansion rate, H , at the redshifts $z = 2.3$ [19] and $z = 2.4$ [20]. More recent studies of the DR11 [21] and DR12 [22] quasars catalogs achieved more precise measurements of these quantities at $z = 2.34$ and $z = 2.33$, respectively (see also [23]).

A common feature in these analyses is the assumption of a fiducial cosmological model to compute the comoving distance among pairs of cosmic sources, and then calculate the 2PCF in order to analyze the probability to find pairs correlated at a given distance scale. In this case, the sample contains both the transversal and the radial BAO modes, and the traditional way to quantify the cosmic evolution is through the spherically-averaged distance, D_V , with mixed information from both modes [12].

Alternatively, we follow a *quasi* model-independent approach to measure the transversal BAO mode at high redshift, and for this we consider a sample of quasars in a thin redshift bin of data from the DR12 of the SDSS [24]. The main idea behind this approach is that, if the redshift bin is sufficiently thin then the two-point angular correlation function (2PACF), calculated without using a fiducial cosmological model, successfully captures the transversal BAO mode. Rigorously, this procedure is *quasi* model-independent because a cosmological model is used just in two steps [25–29]: (i) the transversal BAO analysis is done in a thin but non-null redshift bin, i.e., $\delta z \neq 0$, for this a shift –weakly dependent on a cosmological model– is applied to the measured BAO angular position; however, for the quasars sample in study here, where $\delta z = 0.05$, the shift correction is only 0.9% of the BAO measured scale (as we shall show); (ii) the sound

*Electronic address: edilsonfilho@on.br

†Electronic address: bernui@on.br

‡Electronic address: gabriela@on.br

§Electronic address: camilanovaes@on.br

horizon value, r_s , used to calculate the angular diameter distance from the BAO angular position, D_A , is obtained assuming a cosmological model (see, e.g., [29, 30] for a discussion about this point).

This work is organized as follows. In section II we briefly describe the quasars sample investigated, while in section III we explain the methodology of our analyses. In section IV we present our results, and their discussion and final conclusions are done in section V. We leave to the Appendix section the discussion of our robustness tests.

II. THE QUASARS DATA SET

The data used in this work is part of the twelfth public Data Release Quasar catalog (DR12Q), phase III, from the Sloan Digital Sky Survey (SDSS-III) [31]¹. The complete sample of DR12Q contains 297,301 quasars from the Baryon Oscillation Spectroscopic Survey (BOSS) [32], among which 184,101 have $z \geq 2.15$ (actually, more than 90% of them are new discoveries), covering a total area of $9,376 \text{ deg}^2$ in the sky. The full sample has been spectroscopically confirmed based in a visual inspection of the spectra of each quasar. The SDSS-III/BOSS limiting magnitudes for quasar target selection are $r \leq 21.85$ or $g \leq 22$ [24]. Perhaps, the main challenge faced in the quasar BOSS survey was to obtain a high number-density sample, satisfying the minimum threshold proposed of 15 quasars per square degree [24]. In fact, current sample is actually dense enough to perform the analyses in very thin redshift bins. The methodology followed to arrive to this sample was based in a SDSS pipeline and is fully described in Pâris et al. (2017) [24].

With this exceptional quasars catalog, DR12Q, we search for a statistically significant angular BAO detection. The DR12Q sample is displayed in two disconnected regions of the sky, then we select that one containing the largest amount of quasars, that is, the quasars located in the sky patch with $90^\circ < \alpha < 270^\circ$, where α is the right ascension in equatorial coordinates; moreover, we consider the quasars sample in the redshift range $2.20 - 2.80$. After several analyses, including the evaluation of the statistical significance of the BAO bump in each case, we finally selected the thin shell: $z \in [2.20, 2.25]$, which contains a total of 10,526 quasars.

III. METHODOLOGY

Traditionally, the BAO analyses assume a fiducial cosmology to compute the comoving distance among pairs,

then the characteristic scale is found through the three-dimensional (3D) two-point correlation function. Here instead, we use the two-dimensional (2D) version of this correlation function, that is, the two-point angular correlation function (2PACF), using quasars data in a thin redshift shell. This analysis is only possible now because the current data is dense enough in redshift space to measure the angular BAO signal with high statistical significance.

A. The two-point angular correlation function

The way to characterize the clustering of galaxies, quasars, and other cosmological tracers is through the two-point correlation function (2PCF) [33–37]. The 2PCF is based on counting pairs of cosmic objects in a data set (quasars, for example) $DD(s)$ at a given comoving 3D distance s and compare this with the number of pairs $RR(s)$ from a random set.

The most used 2PCF in astrophysical applications is the Landy-Szalay, LS, estimator [37], which has a better performance when compared with other estimators, because it shows the smallest deviations for a given cumulative probability. Furthermore, the LS estimator is less sensitive to the number of the random points [38]. This estimator is defined by

$$\xi(s) \equiv \frac{DD(s) - 2DR(s) + RR(s)}{RR(s)}, \quad (1)$$

where $DR(s)$ counts the pairs, one in the data set and the other in the random set, separated by a distance s . The quantity $\xi(s)$ gives the probability of finding two points of a data set at a given distance s . If there is an excess of probability to find a characteristic scale, as in the case of acoustic scale, it will appear as a bump in the $\xi(s)$ vs. s plot. The location of the bump indicates the statistically preferred distance between the pairs of the studied sample.

A 3D 2PCF estimator assumes a cosmological model (flat Λ CDM, for example) to calculate the comoving distance s between pairs of the data and the random catalogs. To avoid this model dependence we follow a different approach. We use the two-point angular correlation function 2PACF [2] to estimate the transversal BAO contribution, analysis that is possible to be done selecting the data sample in a sufficiently thin redshift shell δz . The expression for the 2PACF estimator, $\omega(\theta)$, at mean redshift \bar{z} , is given by

$$\omega(\theta) \equiv \frac{DD(\theta) - 2DR(\theta) + RR(\theta)}{RR(\theta)}, \quad (2)$$

with θ , the angular separation between any pair of quasars, given by

$$\theta = \arccos[\sin \delta_A \sin \delta_B + \cos \delta_A \cos \delta_B \cos(\alpha_A - \alpha_B)],$$

¹ www.sdss.org/dr12/algorithms/boos-dr12-quasar-catalog/

where α_A, α_B and δ_A, δ_B are the right ascension and declination coordinates of the quasars A and B , respectively [25, 37, 39].

To find the angular scale of the BAO bump in the 2PACF, θ_{FIT} , we use the method proposed in Sánchez et al., 2011 [25], which is based on the empirical parametrization of $\omega = \omega(\theta)$

$$\omega(\theta) = A + B\theta^\gamma + C \exp^{-(\theta - \theta_{\text{FIT}})/2\sigma_{\text{FIT}}^2}, \quad (3)$$

where $A, B, C, \gamma, \theta_{\text{FIT}}$, and σ_{FIT} are free parameters. Therefore, the best-fit of the 2PACF by this expression provides the BAO bump position, θ_{FIT} , and the width of the bump, σ_{FIT} , define the error associated to the measure θ_{FIT} . The final determination of the acoustic peak is achieved after accounting for an effect that produces a small displacement of the BAO bump, as we discuss below.

The non-null thickness of the shell containing the data, of size δz in redshift space, produces a shift in the acoustic peak due to a *projection effect*. To understand this effect consider first the quasars belonging to a BAO sphere and contributing to the BAO bump in a 3D analysis, where the sphere's centre is located at the redshift \bar{z} (the mean value of the data in the redshift shell, of width δz , in study). In the case of the 2D analysis, the BAO signature in the 2PACF comes from the quasars displayed along circles, or quasi circles, located in the transversal plane (the plane perpendicular to the line-of-sight). This means that, in the 2D analysis, one is assuming that the whole sample of quasars are projected into the plane with redshift \bar{z} . The projection effect produced by this assumption has been studied in detail (see, e.g., [25, 27]) and the net result is a shift in the angular position of the BAO bump, quantity that can be estimated using numerical analysis. Sánchez et al. (2011) have shown that for small δz values and for data at $\bar{z} > 2$, which is our case, the dependence of the shift on the cosmological parameters is negligible. Here below we perform such detailed numerical analysis that confirms this prediction for the quasars sample in analysis.

B. The dependence of the angular BAO scale with the fiducial model

To compute the dependence of the angular BAO scale with the fiducial cosmology one has to perform a numerical integration to evaluate the projection effect on the expected 2PCF, ξ_E . For this, consider a sample of cosmic objects in a thin redshift bin $z \in [z_1, z_2]$, that is, $z_1 \simeq z_2$. Because of this, $\xi_E^{z_1}(s) \simeq \xi_E^{z_2}(s) \simeq \xi_E^{\bar{z}}(s)$, where $\bar{z} \equiv (z_1 + z_2)/2$. Therefore, one can obtain the expected 2PACF, $\omega_E^{\bar{z}}(\theta)$, as a projection of the expected 2PCF, $\xi_E^{\bar{z}}(s)$, in that redshift shell

$$\omega_E^{\bar{z}}(\theta) = \int_0^\infty dz_1 \phi(z_1) \int_0^\infty dz_2 \phi(z_2) \xi_E^{\bar{z}}(s), \quad (4)$$

where ϕ is the top-hat selection function which should be normalized to 1, s is the 3D separation between pairs, and for a spatially flat Robertson-Walker metric is calculated using the relation: $s = \sqrt{\zeta^2(z_1) + \zeta^2(z_2) - 2\zeta(z_1)\zeta(z_2)\cos\theta}$, where θ is the angular separation between those pairs, and $\zeta(z_i)$ is the comoving radial distance to the quasar with redshift z_i , obtained using a cosmological model. The expected 2PCF is given by

$$\xi_E^{\bar{z}}(s) = \int_0^\infty \frac{dk}{2\pi^2} k^2 j_0(ks) P(k, \bar{z}), \quad (5)$$

where j_0 and P are the spherical Bessel function of zero order and the matter power spectrum, respectively. To calculate the matter power spectrum one needs to assume a cosmological model, this is the model dependence step mentioned in section I. However, as we shall confirm in section IV C, for the features of the sample in study, $\bar{z} = 2.225$ and $\delta z = 0.05$, the model dependence of our BAO measurement is actually weak [25].

IV. DATA ANALYSES AND RESULTS

In this section we perform the analysis that lead us to a robust measurement of the angular BAO scale in the DR12Q quasars data sample.

A. The bin-size selection and the statistical significance

Using the estimator of equation (2), we obtained the 2PACF for our quasar sample in the redshift range $z = 2.20 - 2.25$ (mean redshift of $\bar{z} = 2.225$), as presented in figure 1. Note that the 2PACF was estimated for equally spaced values of θ in the range $0^\circ \leq \theta \leq 10^\circ$, in a total of $N_b = 33$ bins. However, to extract the BAO bump information, θ_{FIT} and σ_{FIT} , we fit the equation (3) only to the points in the range $0^\circ < \theta \leq 3.0^\circ$, well beyond the angular BAO scale. The BAO bump is clearly identified at the position $\theta_{\text{FIT}} = 1.83^\circ \pm 0.33^\circ$.

In order to verify the influence of the binning of the angular separation θ to our result, we tested several other number of bins, besides $N_b = 33$ presented in figure 1. These analyses show that θ_{FIT} slightly depends on the choice of the number of bins. The criterion to decide for the best bin number choice is through the statistical significance value in each case. In our analyses, the largest statistical significance was obtained with $N_b = 33$, as can be seen in table I, where we summarize only the three best cases, namely, $N_b = 29, 33$, and 35.

The statistical significance analyses presented here were estimated through χ^2 analyses comparing the 2PACF from the quasars DR12Q data to two best-fit curves: (i) the best-fit of these 2PACF data points by the equation 3 (which provides a χ_1^2 value); and (ii) the

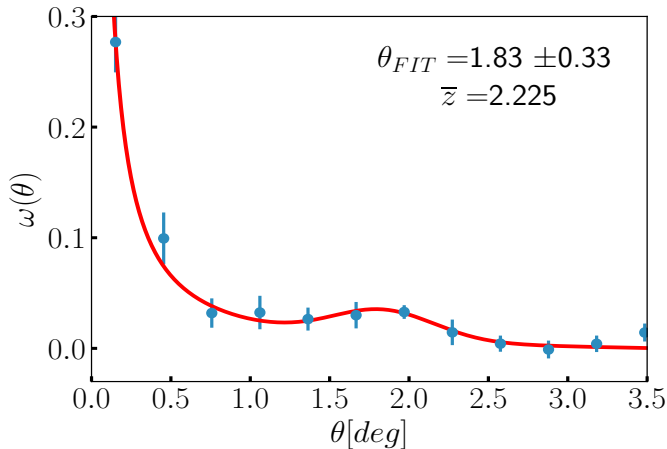


FIG. 1: The 2PACF calculated from the quasars sample DR12Q at $\bar{z} = 2.225$ (dots) and the best-fit curve obtained using the equation (3) (continuous line). In this case we have used $N_b = 33$ (see text for details).

best-fit of the same data, after excluding the points composing the BAO bump, by the power law terms, i.e., $\omega(\theta) = A + B\theta^\gamma$ (which provides a χ^2_2 value). Then, from both χ^2 analyses, we are able to estimate the difference $\Delta\chi^2 = \chi^2_1 - \chi^2_2$ (with 3 degrees of freedom) and, in consequence, also the statistical significance level, as given in the last column of the table I.

N_b	θ_{FIT} [deg]	σ_{FIT} [deg]	stat. sign. [σ]
29	1.74	0.31	3.48
33	1.83	0.33	3.82
35	1.80	0.32	1.88

TABLE I: The θ_{FIT} and σ_{FIT} values obtained for each choice of number of the bins (N_b). The last column displays their corresponding statistical significance.

B. Small shifts in the quasars positions

To show that the BAO bump we found is a robust detection we have performed an important test, namely the *small shifts criterium*, proposed by Carvalho et al. 2016 [27]. This test consists of performing the 2PACF analyses in modified quasars catalogs, that is, instead of the original quasars sample we generate a modified catalog by perturbing slightly the angular positions of the quasars. The main goal of this test is to distinguish the BAO bump, which is expected to be robust and, consequently, survive (or be smoothed) under small perturbations in the quasars positions, instead those bumps sourced by systematic effects would disappear.

For this purpose, we generated 100 2PACFs and then performed their average. Each one of them was calculated by considering a different randomized quasars data catalog obtained in the following way: we change the quasar's angular positions by sorting their new positions using a Gaussian distribution, with mean corresponding to the original positions and with standard deviation equal to 0.10 (0.25 and 0.50) causing largest displacements of $\sim 0.5^\circ$ (1.25° and 2.5°), with respect to the original quasars positions. In the calculation of these 100 2PACF we use the same set of 16 random catalogs used in the analyses done throughout this work, always applying the expression 2.

In figure 2 we displayed the results achieved in these three cases. As observed, the larger the random displacements in the quasars angular positions the smoother the 2PACF curves, destroying the BAO bump signature. Simultaneously, these displacements also smooth other maxima and minima, possible coming from systematic effects, appearing in the original 2PACF.

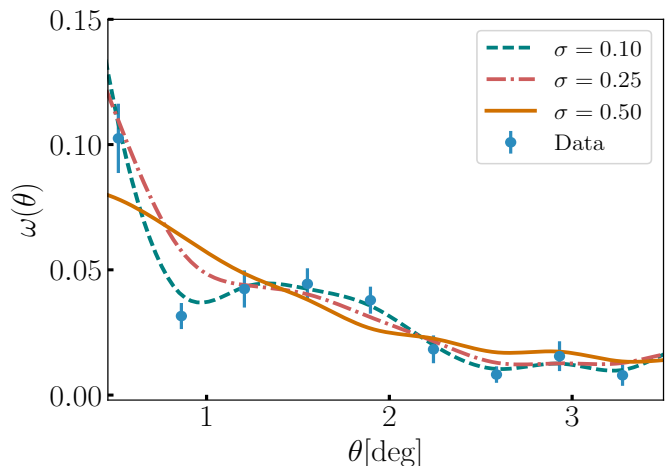


FIG. 2: The 2PACF of the new angular position data which was shifted by a random amount from the quasars data following Gaussian distribution with $\sigma = 0.10, 0.25$, and 0.50 (the continuous, dashed and dotted lines, respectively). The big dots represent the original data. In this plot we used $N_b = 29$.

C. The projection effect

To quantify the BAO bump shift due to the projection effect we need to compute the expected angular BAO scale, θ_E^0 , which corresponds to the bump position when one computes the 2PACF using the equation (4) for the case of $\delta z = 0$. Next, one applies the same procedure but considering $\delta z = 0.05$, which is the thickness of the redshift shell used in the current acoustic peak measurement, to find $\theta_E^{\delta z}$. Then, the BAO angular scale, θ_{BAO} , is

given by

$$\theta_{\text{BAO}}(\bar{z}) = \theta_{\text{FIT}}(\bar{z}) + \Delta\theta(\bar{z}, \delta z), \quad (6)$$

where $\Delta\theta(\bar{z}, \delta z) \equiv \theta_E^0 - \theta_E^{\delta z}$, that is, once we compute the expected values θ_E^0 and $\theta_E^{\delta z}$, we finally perform the shift in the measured value $\theta_{\text{FIT}}(\bar{z})$ to find the BAO angular scale $\theta_{\text{BAO}}(\bar{z})$.

This numerical analysis assumes six cosmological parameters: the baryon density $\omega_b = \Omega_b h^2$, the cold dark matter density $\omega_c = \Omega_c h^2$, the ratio between the sound horizon and the angular diameter distance at decoupling Θ , the optical depth to reionization τ , the overall normalization of the primordial power spectrum \mathcal{A}_s , and the effective tilt n_s . As a reference model we use $\omega_b h^2 = 0.0226$, $\omega_c h^2 = 0.112$, $\Theta = 1.04$, $\tau = 0.09$, $\mathcal{A}_s e^9 = 2.2$, $n_s = 0.96$, with $H_0 = 100h$ km/s/Mpc. We also assume flatness and set the neutrino masses equal to 3.046 eV.

Using this reference model we find the values $\theta_E^0 = 1.518^\circ$ for $\delta z = 0$ and $\theta_E^{\delta z} = 1.504^\circ$ for $\delta z = 0.05$. The shift obtained is 0.014° , i.e., the projection effect is almost negligible since it produces a shift in the BAO angular position of 0.9%.

D. Cosmological constraints

Here we measured a new angular acoustic scale, θ_{BAO} at $\bar{z} = 2.225$. We combine this new measure with other eight data points provided by [27, 29] (obtained following the same quasi-independent model approach) to constrain parameters in the cosmological models with constant and variable equations of state, namely wCDM and w(a)CDM models.

For the w(a)CDM model we assume the Barboza-Alcaniz parametrized equation of state [40]: $w(a) = w_0 + w_a [(1-a)/(2a^2 - 2a + 1)]$. The relation between the angular BAO scale, θ_{BAO} , and the angular diameter distance, D_A , is obtained using the expression

$$\theta_{\text{BAO}}(z) = \frac{r_s(z_{\text{drag}})}{(1+z)D_A(z)}, \quad (7)$$

where $r_s(z_{\text{drag}})$ is the sound horizon at the end of baryon drag, and is provided by CMB measurements. To constrain the cosmological parameters we combine the transversal BAO data with the CMB shift parameter information defined as $R \equiv \sqrt{\Omega_m H_0^2} r_s(z_{\text{rec}})$, where $r_s(z_{\text{rec}})$ is the comoving sound horizon at recombination. In our case, we use the shift parameter given by the Planck collaboration $R = 1.7407 \pm 0.0094$ [41].

Assuming the sound horizon value obtained by WMAP9 [42], $r_s = 106.61 \pm 3.47$ Mpc/h, jointly to the Planck measurement of the shift parameter², we constrain the Ω_m and w_0 for the wCDM model. Thus,

the best-fit corresponds to $\Omega_m = 0.31 \pm 0.02$ and $w_0 = -0.92 \pm 0.06$ for the wCDM model, while for w(a)CDM we found $w_0 = -0.87 \pm 0.13$ and $w_a = -0.15 \pm 0.32$. The confidence level contours for $\Omega_m - w_0$ for wCDM model and $w_0 - w_a$ for w(a)CDM model can be seen in figure 3.

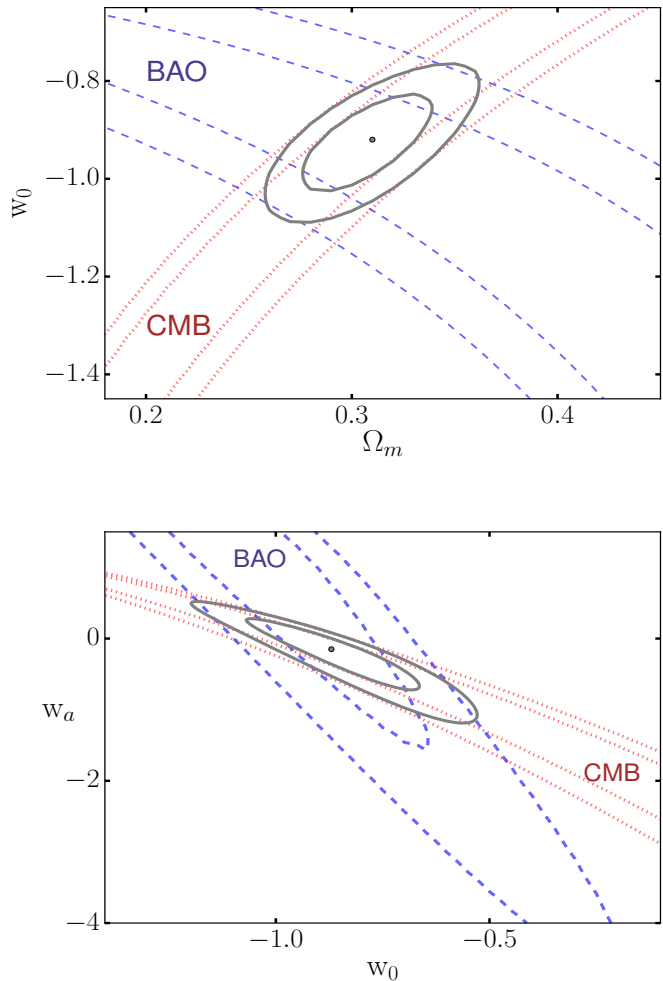


FIG. 3: Confidence level contours of the $\Omega_m - w_0$ and $w_0 - w_a$ planes for the wCDM and w(a)CDM models, respectively.

V. CONCLUSIONS AND FINAL REMARKS

Following the same quasi model-independent approach used in the refs. [27, 29, 43], we obtained a robust and statistically significant measurement of the BAO angular scale, $\theta_{\text{BAO}} = 1.85^\circ \pm 0.33^\circ$ at $\bar{z} = 2.225$, using the superb quasars catalog DR12Q of the SDSS collaboration. With

² We use these values from different surveys because they are ex-

pected to be non-correlated data, therefore the current analysis is valid.

this, we have increased the number of available BAO angular scale data, but this time with a measurement at high redshift.

After measuring the acoustic peak position through the 2PACF, it was necessary to apply a shift correction due to unavoidable projection effects due to the non-null thickness of the redshift shell, $\delta z \neq 0$, of the quasars sample. But, as expected from previous analyses [25], the numerical evaluation of this effect showed a negligible shift correction of less than 1%, evidencing a weak dependence of our measurement with respect to the reference cosmological model. At the same time, one observes that the effective model contribution in this approach comes from the sound horizon value, r_s , which is derived from CMB measurements in a model-dependent way [42].

It is worth to say that we validated our angular BAO detection through diverse robustness tests. In fact, we show in section IV A that the BAO signal is also robust under diverse bin-size choices, N_b , used in the calculation of the 2PACF and the corresponding BAO scale measurement. Additionally, we verify in section IV B that our measurement is stable under small Gaussian random perturbations of the angular positions of the quasars sample (this is a useful procedure which also leads to discriminate noise bumps from the true BAO signature). Moreover, in the Appendix section, we reproduce the 2PACF analyses but this time considering diverse number of random sets, namely, 16, 25, and 50 samples, obtaining the same result, just with slightly different error bars, as shown in the Appendix section.

Finally, we combined this new high redshift angular BAO measurement with other eight data points (from refs. [27, 29]) to constrain the cosmological parameters from Λ CDM and $w(a)$ CDM models. As observed, our results show an excellent agreement with the standard cosmological model Λ CDM: the best-fit corresponds to $\Omega_m = 0.31 \pm 0.02$ and $w_0 = -0.92 \pm 0.06$ for the w CDM model, while for $w(a)$ CDM we found $w_0 = -0.87 \pm 0.13$ and $w_a = -0.15 \pm 0.32$ (see figure 3 and section IV D for details).

Acknowledgements

We are grateful to Joel C. Carvalho for his support in numerical programming, and to him and Jailson Alcaniz for insightful discussions. The authors thank CAPES and CNPq for the financial support. We also acknowledge a CAPES PVE project (88881.064966/2014-01) within the *Science without Borders Program*. CPN was partially supported by the DTI-PCI program of the Brazilian Ministry of Science, Technology, and Innovation (MCTI). CPN also acknowledges FAPERJ (Pós-doc Nota 10).

Appendix A: The Random Catalog Generator

A crucial part in the robust, and statistically significant, detection of the BAO angular scale is the production of a set of random catalogs with the same features as the observed quasars catalog: they should contain cosmic objects distributed in the same geometry of the survey, and their number should be equal to the number of objects in the data catalog.

The methodology we use to generate our random catalogs, in order to obtain a homogeneous Poisson distribution of cosmic objects [33], was to shuffle the original data in a way that any possible correlation in the data would be destroyed [44]. There are many approaches to produce these simulated data, but perhaps the most important task is to test their performance, and the simplest way to do this is through a *null test* (see, e.g., section 5 in ref. [37]). Consider that we have produced $N + 1$ random catalogs. A null test considers any of the randoms catalog as the *pseudo-data-catalog* and performs the 2PACF, using the equation (2), with the remaining N random catalogs. Since there is no preferred clustering at any scale, the expected 2PACF is, up to the error bars, a null correlation, that is, one does not expect angular correlations at any scale between a *pseudo-data-catalog* and a set of N random catalogs.

We performed this test considering three cases: $N = 16, 25, \text{ and } 50$, and our results are displayed in figure 4. As observed, they show an excellent performance, leading us to conclude that our random catalogs are actually suitable for the 2PACF analyses we performed.

Another important robustness test concerns the appropriate number of random catalogs to be used in the 2PACF analyses, in a way that one can ensure that our detection was not fortuitous, but a consequence of a well-established approach. Our detection of the BAO bump was first made using $N = 16$ random catalogs, but after that we have performed complementary analyses considering the cases with $N = 25$ and 50 random catalogs. Our results are displayed in figure 5, where one observes that there is no clear evidence of a benefit in any of the cases. Subsequently, we have investigated the statistical significance of the BAO bump detections in these three cases, namely, considering $N = 16, 25, \text{ and } 50$. Our analyses indicate that the statistical significance of the BAO angular scale in each case does not improve the measurement with a larger number of random data, in fact we obtained: $3.82\sigma, 1.84\sigma, \text{ and } 2.02\sigma$ for these three cases, respectively.

All these tests lead us to conclude that the BAO angular scale here obtained is, in fact, a robust and statistically significant detection.

[1] Ade, P. A. R., et al., 2016, A&A 594, A13.

[2] Peebles, P. J. E. and Yu, J. T., 1970, Astrophys. J., 162,

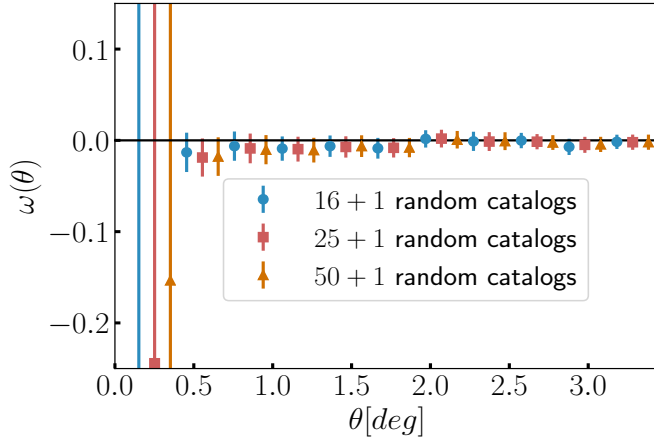


FIG. 4: The 2PACF obtained through $N = 17$ (dots), 26 (squares), and 51 (triangles) random catalogs, where the last random catalog in each sample was considered as the *pseudo-data-catalog* (see the text for details). The second and third data points were artificially shifted to the right by 0.10° and 0.20° , respectively, for clarity.

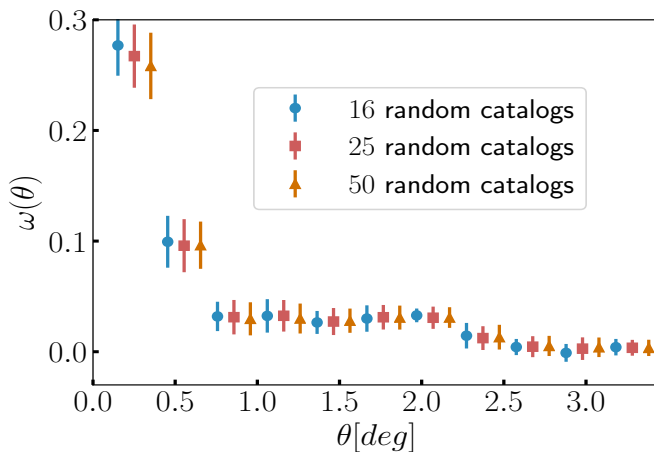


FIG. 5: Comparison of the 2PACF ($N_b = 33$) for the DR12Q data sample (10,526 quasars with $\bar{z} = 2.225$) using $N = 16$ (dots), 25 (squares) and 50 (triangles) random catalogs. The second and third data points were artificially shifted to the right by 0.10° and 0.20° , respectively, for clarity.

815.

- [3] Sunyaev, R. A. and Zeldovich, Y. B., 1970, *Astrophys. Space Sci.*, 7, 3.
- [4] Seo, H.-J. and Eisenstein, D. J., 2003, *Astrophys. J.* 598, 720.
- [5] Weinberg, D. H., Mortonson, M. J., Eisenstein, D. J., Hirata, C., Riess, A. G., Rozo, E., 2013, *Phys. Rept.*, 530, 87.
- [6] Eisenstein, D. J., Hu W., 1998, *Astrophys. J.*, 496, 605.

- [7] Meiksin, A., Martin White, J. A. Peacock, 1999, *Monthly Notices of the Royal Astronomical Society*, 304, 851.
- [8] York, D. G. *et al.*, 2000, *Astronom. J.*, 120, 1579.
- [9] Blake, C. *et al.*, 2011, *Monthly Notices of the Royal Astronomical Society*, 418, 1707.
- [10] Beutler, F. *et al.*, 2011, *Monthly Notices of the Royal Astronomical Society*, 416, 3017.
- [11] Cole, S. *et al.* [2dFGRS Collaboration], 2005, *Monthly Notices of the Royal Astronomical Society*, 362, 505.
- [12] Eisenstein, D. J. *et al.* (SDSS Collaboration), 2005, *Astrophys. J.*, 633, 560-574.
- [13] Wang, Y. *et al.*, 2016, arXiv:1607.03154.
- [14] Hong, T., Han, J. L., Wen, Z. L., Sun, L., Zhan, H., 2012, *Astrophysical Journal*, 749, 81.
- [15] Veropalumbo, A., Marulli, F., Moscardini, L., Moresco, M., Cimatti, A., 2014, *Monthly Notices of the Royal Astronomical Society*, 442, 3275.
- [16] White, Martin, 2003. arXiv preprint astro-ph/0305474.
- [17] McDonald, P., 2003, *Astrophys. J.* 585, 34.
- [18] Bassett, B., Hlozek, R., 2009, arXiv:0910.5224.
- [19] Busca, N., *et al.*, 2013, *A&A*, 552, A96.
- [20] Slosar, A., *et al.*, 2013, *Journal of Cosmology and Astroparticle Physics* 2013, 026.
- [21] Delubac, T., *et al.*, 2015, *A&A*, 574, A59.
- [22] Bautista, J. E. *et al.*, 2017, arXiv:1702.00176.
- [23] Ata, M., *et al.*, 2017, arXiv:1705.06373
- [24] Pâris, I., *et al.*, 2017, *A&A*, 597, A79.
- [25] Sánchez E. *et al.*, 2011, *Monthly Notices of the Royal Astronomical Society*, 411, 277.
- [26] Carnero, A. *et al.*, 2012, *Monthly Notices of the Royal Astronomical Society*, 419, 1689.
- [27] Carvalho, G. C. *et al.*, 2016, *Phys. Rev. D*, 93, 023530.
- [28] Salazar-Albornoz, S., Sánchez, A. G., Padilla N. D., Baugh C. M., 2014, *Monthly Notices of the Royal Astronomical Society*, 443, 3612.
- [29] Alcaniz, J. S., *et al.*, 2016, arXiv:1611.08458.
- [30] Heavens, A., Jiménez, R., Verde, L., 2014, *Phys. Rev. Lett.*, 113, 241302.
- [31] Eisenstein, D. J., Weinberg, D. H., Agol, E., *et al.*, 2011, *Astrophys. J.*, 142, 72.
- [32] Dawson, K. S., Schlegel, D. J., Ahn, C. P., *et al.*, 2013, *Astronom. J.*, 145, 10.
- [33] Peebles, P. J. E., Hauser M. G., 1974, *Astrophys. J. Suppl.*, 28, 19.
- [34] Davis, M., Peebles, P. J. E., 1983, *Astrophys. J.*, 267, 465.
- [35] Hewett, P. C., 1982, *Monthly Notices of the Royal Astronomical Society*, 201, 867.
- [36] Hamilton, A. J. S. 1993, *Astrophys. J.*, 417, 19.
- [37] Landy, S. D., Szalay A. S., 1993, *Astrophys. J.*, 412, 64.
- [38] Kerscher, M., Szapudi I., Szalay A. S., 2000, *Astrophys. J. Lett.*, 535, L13.
- [39] Crocce, M., Cabré A., Gaztañaga E., 2011, *Monthly Notices of the Royal Astronomical Society*, 414, 329.
- [40] Barboza, E. M., Alcaniz, J. S., 2008, *Physics Letters B* 666, 415.
- [41] Wang, Y., Wang, S., 2013, *Phys. Rev. D* 88, 043522.
- [42] Hinshaw, G., *et al.*, 2013, *Astrophys. J. Suppl.*, 208, 19.
- [43] Carvalho, G. C. *et al.*, in preparation.
- [44] Rego, C. R. C., Frota, H. O., Gushima, M. S., 2013, *Journal of Hydrology* 495, 208.